〈일반논문〉
Journal of the Korean Society of Visualization, Vol. 20, No. 3 (74~85), 2022
(Manuscript received : 2022.10.07./Revised : 2022.11.06./Accepted : 2022.11.10.)
DOI:http://dx.doi.org/10.5407/jksv.2022.20.3.074

ISSN 1598-8430 Print
ISSN 2093-808X Online

이류확산 방정식 계산을 위한 입방보간유사입자 격자볼츠만 모델

김미래* · 첸빙키** · 김경천†

The Cubic-Interpolated Pseudo-Particle Lattice Boltzmann Advection-Diffusion Model

Mirae Kim*, Binqi Chen** and Kyung Chun Kim†

Abstract We propose a Cubic-Interpolated Pseudo-Particle Lattice Boltzmann method (CIP-LBM) for the convection-diffusion equation (CDE) based on the Bhatnagar-Gross-Krook (BGK) scheme equation. The CIP-LBM relies on an accurate numerical lattice equilibrium particle distribution function on the advection term and the use of a splitting technique to solve the Lattice Boltzmann equation. Different schemes of lattice spaces such as D1Q3, D2Q5, and D2Q9 have been used for simulating a variety of problems described by the CDE. All simulations were carried out using the BGK model, although another LB scheme based on a collision term like two-relation time or multi-relaxation time can be easily applied. To show quantitative agreement, the results of the proposed model are compared with an analytical solution.

Key Words : Lattice Boltzmann Method(격자볼츠만법), Cubic-Interpolated Pseudo-Particle(입방 보간 유사 입자), Single relaxation time (단일 완화 시간), Advection-Diffusion(이류 확산), Convection-Diffusion Equation(대류 확산 방정식)

1. Introduction

In the last two decades, interest has gradually been increasing in using a modern numerical technique for understanding the physics of advection-diffusion or convection-diffusion transport phenomena. The Lattice Boltzmann method (LBM) lies between the finite difference algorithm and the lattice gas scheme because it can solve a microscopic kinetic equation, which has been useful in the field of fluid dynamics. The LBM has many advantages over other traditional techniques for obtaining solutions of partial differential equations, but the main benefits of this method are the ease of implementation, explicitness, and the capability of working in a parallel computation domain, which results in very fast codes because the physical interpretation of the scheme is well suited for implementation on massively parallel.[1-3]

In addition, the LBM has been extended to deal with complex geometries and solve the convection-diffusion equation.[4] Dawson et al. were the first

† Rolls-Royce and Pusan National University Technology Center in Korea, Research Professor
E-mail: kckim@pusan.ac.kr
* School of Mechanical Engineering, PNU, Research Professor
** School of Aeronautics and Astronautics, University of Electronic Science and Technology of China, Associate Professor

to use the LBM to simulate solvent flow instead of solving Navier-Stokes equations.[1] The capabilities of the LBM have been proven to simulate pure diffusion, homogeneous chemical reactions, and pattern formation by comparing with theoretical predictions of the macroscopic reaction-diffusion equations. Van der Sman and Ernst applied irregular lattices in the

LBM for convection-diffusion equation in order to improve the efficiency of the proposed model for solving the CDE for the concentration field.[5] They showed that the LBM had equivalent performance by comparing their scheme with numerical models based on N-S equations (like finite element and finite difference methods). However, a mass-conserving equilibrium distribution function cannot be obtained because the BGK scheme has only one relaxation time for each lattice vector.[6] In order to improve the stability and keep the accuracy of simulating anisotropic CDE problems, a few versions of collision have been proposed, as multi-relaxation time and two-relaxation time.[7-8]

Several LB models have been suggested for modeling the CDE, which can be correctly modeled under some idealistic assumptions (e.g., constant velocity). In general, all the models are placed in three classifications that can be used to resolve the convection-diffusion equation. The first is passive scalar models, in which the first component represents the fluid motion and the second component simulates a passive concentration field where the concentration field must satisfy the passive-scalar equation.[9] The second is multi-speed models, which can be managed with particle velocities linking to its nearest neighbor's lattice. However, this method is not linearly stable in the limit of low transport coefficients.[10] The third type of LBM model of advective and diffusive transport is double-distribution functions, which are the most stable and accurate schemes.[11-12]

We propose a double-distribution function in the Cubic-Interpolated Pseudo-Particle LBM (CIP-LBM). This scheme presents the evolution of mass and momentum and the solute transport separately by using two different distribution functions. This model is computationally robust and applicable to problems with different Peclet numbers. In addition, this model directly simulates the change of transport of a dilute solute and involves a low-order moment that provides higher numerical stability than passive-scalar and multi-speed models. In order to validate the model for recovering the CDE, some numerical examples are presented to demonstrate the capability of the model with different microscopic velocities. CIP-LBM simulations for turbulent flow are possible. However, we have limited to the laminar flow because most of convection-diffusion problem is within laminar regime because the time scales for convection and diffusion should be equal.

2. Method

2.1 The LBM method

The Bhatnagar-Gross-Krook (BGK) LBM is based on two distribution functions that are applied for the momentum equation and solute transport. The Bhatnagar-Gross-Krook (BGK) collision model is used to model collisions as a statistical redistribution of momentum which locally drives the system toward equilibrium while conserving mass and momentum. However, one of the major problems when it related with the Boltzmann equation is the complicated nature of the collision integral. Collision operator represents the change in distribution function per unit time due to collision. In BGK, the main effect of the collision term is to bring the density distribution function closer to the equilibrium distribution.

Macroscopic fluid quantities such as concentration

and velocity are obtained by solving the momentum and solute distributions. In the double distribution function (DDF) approach, the first component is used for fluid flow, and the solute component has no velocity of its own. Therefore, the solute component is carried by the background fluid. The governing equation of the DDF model for the CDE is given by:

$$\frac{\partial \phi_i^1(\boldsymbol{x},t)}{\partial t} + \boldsymbol{c}.\nabla\phi_i^1(\boldsymbol{x},t) = \Omega_i^1(\boldsymbol{x},t) + F_i(\boldsymbol{x},t) \qquad (1)$$

$$\frac{\partial \phi_j^2(\boldsymbol{x},t)}{\partial t} + \boldsymbol{c}.\nabla\phi_j^2(\boldsymbol{x},t) = \Omega_j^2(\boldsymbol{x},t) + R_j(\boldsymbol{x},t) \qquad (2)$$

where ϕ^l is the distribution function of momentum for particle velocity c in the space direction $\boldsymbol{x}$ and time $\boldsymbol{t}$. ϕ^2 is the solute component in microscopic quantity, while i and j denote the microscopic velocities of the momentum and solute component, respectively.

In general, the LBM equation consists of two steps: a collision term (right-hand side) that describes the collision of the particle distribution function, and a streaming term (left-hand side), which represents the propagation of the distribution function after the collision term. The magnitude of an external force $F(\boldsymbol{x}, t)$ (such as gravity or the mass change caused by chemical reaction) can act either on the main fluid component in Eq. (1) or can be incorporated in a velocity term.[13] $R(\boldsymbol{x}, t)$ is the source term and can be found in some published works.[14] There are a few schemes of the collision term in the literature. However, the most efficient one is the BGK collision model because of its simplicity and low cost of computation. The BGK model has single relation time, and the equation is given by[13]:

$$\Omega_k^n = -\frac{\phi_k^n(\boldsymbol{x},t) - \check{\phi}_k^n(\boldsymbol{x},t)}{\tau_n} \quad \begin{cases} k = i,j \\ n = 1,2 \end{cases} \qquad (3)$$

$$\check{\phi}_k^n(\boldsymbol{x},t) = \omega_i^n \phi^n \left[1 + \frac{\boldsymbol{e_i}\cdot\boldsymbol{u}}{c_s^2} + \frac{(\boldsymbol{e_i}\cdot\boldsymbol{u})^2}{2c_s^4} - \frac{\boldsymbol{u}\cdot\boldsymbol{u}}{2c_s^2}\right] \qquad (4)$$

where ϕ is a scalar parameter such as species concentration or density at each local node. ϕ can be calculated as the summation of all distribution functions of component n.

$$\phi^n = \sum\nolimits_i \phi_i^n \quad n = 1,2 \qquad (5)$$

$$\phi \cdot \boldsymbol{u} = \sum\nolimits_i \boldsymbol{e_i}\cdot\phi_i^1 \qquad (6)$$

$\check{\phi}$ is the local equilibrium distribution function associated with time t and position $\boldsymbol{x}$, and ω_i is a weight coefficient that satisfies the following conditions:

$$\sum\nolimits_i \omega_i = 1, \ \sum\nolimits_i \omega_i \boldsymbol{e_i} = 0 \qquad (7)$$

We use three common terminologies to refer to the dimension of problem and the number of linkages: D1Q3, D2Q5, and D2Q9. For D1Q3, there are three lattice velocity vectors in one dimension e_x = [-1 0 1] associated with a unique linkage length and time step, and the weighting factors ω_i are 4/6, 1/6, and 1/6. D2Q5 or a four-bit velocity vector and D2Q9 or nine-microscopic velocities are very common for solving the CDE and fluid flow, respectively. D1Q3 model is for one dimensional flow model and two velocity vectors issued from the central node. D2Q5 model has four velocity vectors issued from the central nodes, one of the particle resides at the central node, hence its speed is zero, noted as c(0,0). The distribution function f1 and f2 move with c(1,0) and c(-1,0) (to the east and west), respectively, while f3 and f4 move with speed c(0,1)and c(0,-1)(to the north and south), respectively. Note that it is assumed that $\Delta t = \Delta y = \Delta t$. D2Q9 model is very common, especially for

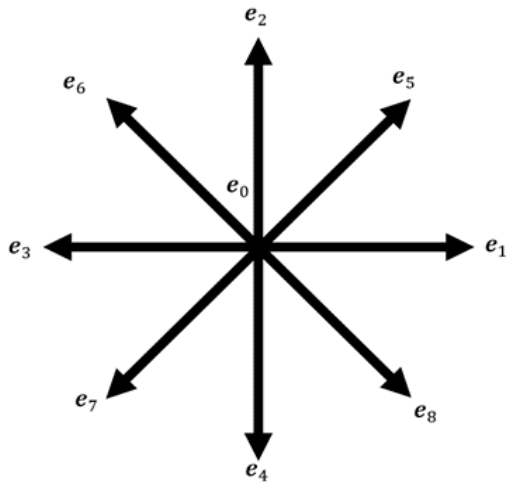

Fig. 1. D2Q9 velocity vectors structure

solving fluid problems. Fig. 1 shows the D2Q9 velocity vectors structure. It has high velocity vectors, with the central particle speed being zero. The speed are c(0,0), c(1,0), c(0,1), c(-1,0), c(0,-1), c(1,1), c(-1,1), c(-1,-1) and c(1,-1) for f0, f1, f2, f3, f4, f5, f6, f7, f8 and f9, respectively. The weight factors for corresponding distribution functions are 4/9, 1/9, 1/9, 1/9, 1/9, 1/36, 1/36, 1/36 and 1/36. Lattice Boltzmann method based on D2Q9 lattice spaces with associated with the Bhatnagar-Gross-Krook (BGK) collision term is proposed to solve the convection-diffusion equation.

The speed vector and the weight factors for both lattice arrangements are:

D2Q5:

$$\boldsymbol{e} = \begin{bmatrix} 0 & 1 & -1 & 0 & 0 \\ 0 & 0 & 0 & 1 & -1 \end{bmatrix}, \quad \omega = \begin{bmatrix} \frac{1}{3} & \frac{1}{6} & \frac{1}{6} & \frac{1}{6} & \frac{1}{6} \end{bmatrix} \tag{8}$$

D2Q9:

$$\boldsymbol{e} = \begin{bmatrix} 0 & 1 & 0 & -1 & 0 & 1 & -1 & -1 & 1 \\ 0 & 0 & 1 & 0 & -1 & 1 & 1 & -1 & -1 \end{bmatrix}, \quad \omega = \begin{bmatrix} \frac{4}{9} & \frac{1}{9} & \frac{1}{9} & \frac{1}{9} & \frac{1}{9} & \frac{1}{36} & \frac{1}{36} & \frac{1}{36} & \frac{1}{36} \end{bmatrix} \tag{9}$$

Through Chapman-Enskohg expansion, we can obtain the diffusion coefficient D and shear stress v in lattice units from the incompressible N-S equations associated with the single dimensionless relaxation time τ_n for each component[10]:

$$\tau_1 = 3v + \frac{1}{2}, \ \tau_2 = 3D + \frac{1}{2} \tag{10}$$

2.2 The CIP model

During the last three decades, the Lattice Boltzmann method (LBM) has proved its capability to simulate a large variety of fluid flows. The CIP-LBM has many advantages over other traditional techniques for obtaining solutions of partial differential equations, but the main benefits of this method are the ease of implementation, explicitness, and the capability of working in a parallel computation domain, which results in very fast codes because the physical interpretation of the scheme is well suited for implementation on massively parallel computers.

The CIP model is applied in the propagation step of the LBM after the collision term, and the analytical solution of the streaming term is:

$$\phi_i^n(\boldsymbol{x} + \boldsymbol{c}_i\delta t, t + \delta t) = \phi_i^{n+}(\boldsymbol{x}, t), \quad \{n = 1,2\} \tag{11}$$

where is the post-collision distribution function at $\boldsymbol{x}$ and t. In order to describe the CIP model, one-dimensional lattice Boltzmann is explained in this section. The Linear equilibrium hyperbolic equation after applying the collision is:

$$\frac{\partial \phi_i^n(\boldsymbol{x}, t)}{\partial t} + \boldsymbol{c}.\nabla\phi_i^n(\boldsymbol{x}, t) = 0, \ \{n = 1,2\} \tag{12}$$

where the constant micro-velocity (c) is assumed to be one. The novelty of applying CIP approximation

is that it can estimate the time evolution of both the distribution function (ϕ) and the derivative of the distribution function, $\bar{\phi}_i^n(\boldsymbol{x},t)=\frac{\partial}{\partial x}\left(\phi_i^n(\boldsymbol{x},t)\right)$ with spatial space (x). Also, the profile of each component is specialized at each node. With this restraint, arithmetical dispersion can be reduced significantly.

The approximate functional form of the gradient of the quantities in the grid interval using cubic-polynomial interpolation is[15]:

$$\Phi^n(x,\phi,\bar{\phi})=\alpha_i(x,\phi,\bar{\phi})\xi_i^{\,3}+\beta_i(x,\phi,\bar{\phi})\xi_i^{\,2}+\bar{\phi}_i^n(x,t)\xi+\phi_i^n(x,t) \tag{13}$$

$$\bar{\Phi}^n(x,\phi,\bar{\phi})=\frac{\partial}{\partial x}\left(\Phi_i^n(\boldsymbol{x},t)\right)=3\alpha_i(x,\phi,\bar{\phi})\xi_i^{\,2}+2\beta_i(x,\phi,\bar{\phi})\xi_i+\bar{\phi}_i^n(x,t) \tag{14}$$

where $\xi=\boldsymbol{e_i}\delta t$ is the constant distance between two neighbor lattices (for example, $\xi=x_i-x_{i-1}$). The coefficients of α_i and β_i can be described in terms of the distribution function and its derivative as:

$$\alpha_i=(\bar{\phi}_i^n+\bar{\phi}_{i-1}^n)\xi^{-2}-2\left(\phi_i^n(x,t)-\phi_{i-1}^n(x,t)\right)\xi^{-3} \tag{15}$$

$$\beta_i=(2\bar{\phi}_i^n+\bar{\phi}_{i-1}^n)\xi^{-1}-3\left(\phi_i^n(x,t)-\phi_{i-1}^n(x,t)\right)\xi^{-2} \tag{16}$$

Once all $\bar{\phi}_i^n$ and ϕ_i^n are given, the value of the right-hand side of Eq. (11) is determined. Then, all the advected profiles of lattice propagation for all grid intervals can be obtained as:

$$\phi_i^{n+}(\boldsymbol{x},t)=\Phi_i^n(x_i+\xi),\quad \bar{\phi}_i^{n+}(\boldsymbol{x},t)=\bar{\Phi}_i^n(x_i+\xi) \tag{17}$$

3. Results and discussion

In order to test the capability of the proposed model for CDE, some examples are presented. These include a conditional probability distribution function, bonded plane source with extended initial sources, 2D plane source, and the problem in the Poiseuille flow. Steady state is reached if the following convergent condition is fulfilled:

$$\frac{\sum_i(|\phi(\boldsymbol{i},t+10\delta t)-\phi(\boldsymbol{i},t)|)}{\sum_i\phi(\boldsymbol{i},t)}\le Tol_{lb} \tag{18}$$

where Tol_{lb} is a tolerance set to 10^{-8}. In order to test the accuracy of the proposed LBM model for the CDE, the relative error (Err) is defined as:

$$\frac{\sum_i\left(\left|\phi(\boldsymbol{i},t)_{analytical}-\phi(\boldsymbol{i},t)_{numerical}\right|\right)}{\sum_i\phi(\boldsymbol{i},t)_{analytical}}=Err_{lb} \tag{19}$$

In simulations, various boundary conditions for the components are identical: bounce back, specified velocity, constant concentration, and an open boundary condition.

The performance and robustness of developed CIP-LBM model were validated by comparison with known analytical solutions. They are one-dimensional (D1Q3) and two-dimensional mass diffusion problem (D2Q5). We first consider one-dimensional diffusion in a finite domain of length L and in which all the diffusing substance is initially concentrated in a plane. Then we extended to two-dimensional mass diffsion problem (D2Q5) with bounded domain. The Poiseuille flow is the last problem tested to demonstrate the capability of the present model for solute transport (D2Q9). For a better comparison, all the variables are normalized.

3.1 Time-dependent distribution function

Probability distributions are normally classified in relations of the probability density function (PDF).

However, a number of probability functions are used in applications such as earthquake prediction, medicine diffusion, and air-conditioning.[16-18] For a continuous function, the PDF is the probability that the variate has the value x. Since the probability at a single point is zero for continuous distributions, it is often expressed in terms of an integral between two points. The normal distribution is a very common probability distribution because it is important in statistics and in natural and social sciences. It is used to represent real-valued random variables with unknown distributions. The probability for an outcome cannot be estimated precisely in such cases, but instead, a probability for a range of outcomes can be determined. In order to apply the LBM, we assume the PDF is a time-dependent distribution function with variance σ^2 that is linear with respect to time:

$$\sigma^2 = \frac{N_{itr} D \delta t}{2} \tag{20}$$

$$\int_a^b f(x|\sigma,\mu)dx = Pr[a \le X \le b] \tag{21}$$

where *f(x)* is a normal distribution, μ is the expectation of the distribution, and N_{itr} is the number of iterations.

The cumulative distribution function (CDF) is another important distribution function that is used to determine the probability of a response being lower than a certain value, higher than a certain value, or between two values. The CDF gives the area under the probability density function up to a specified value and can be obtained from the PDF:

$$F(x) = \int_{-\infty}^{x} f(\mu)d\mu \tag{22}$$

The inverse of the cumulative distribution function is the percent point function (PPF), which shows a distribution function for which a variable is less than or equal to x for a given x. Mathematically, this can be expressed as:

$$Pr[X \le G(\alpha)] = \alpha \tag{23}$$

We used the proposed LBM model to obtain the normal distribution function (bell curve). We used

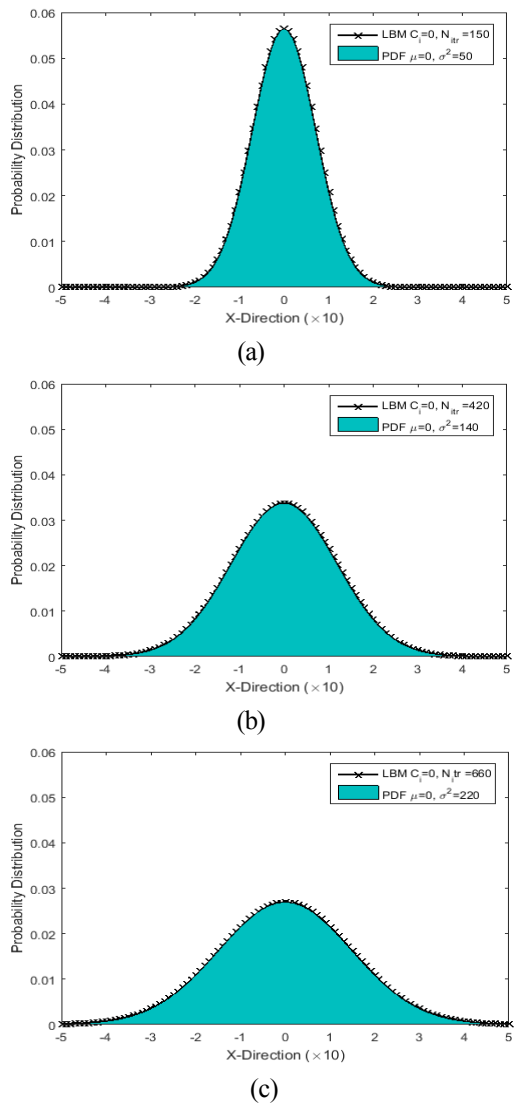

Fig. 2. Probability density function of a normal distribution using LBM. Uniform initial concentration and mean value are zero.

the D1Q2 scheme (a one-dimensional model with two discrete velocities) and a periodic geometry size L_{lbm} and compared it with a mathematical model. The simulations were suspended after reaching an expected variance values of 50, 140, and 220. The lattice Boltzmann parameters are $\tau_\phi = 1$ and $L_{lbm} = 51$, which is fine enough to derive accurate results.

The results of the simulations are plotted against the appropriate analytical solutions in Fig. 2. The numerical results of scalar ϕ are in good agreement with the corresponding analytical solution. As shown in Fig. 2, a normal distribution with any deviation σ is symmetric around the point $x = 0$, which is also where the median and the mean of the distribution equal zero the simulation steps. Additionally, the center of the curve is located at $x = \mu$, where the area under the curve in the range of $x < \mu$ has the same value as the area

where $x > \mu$. The symmetric shape of the distribution function is unimodal, and the maximum value of the probability distribution occurs at $x = \mu$ (Fig. 3). Fig. 4 shows the exact and numerical solutions of the cumulative distribution function (Fig. 4(a)) and the percent point function of the PDF (Fig. 4(b)) at times 150, 420, and 660 in lattice units.

For quantitative evaluation of the accuracy, we calculated the relative errors for different lattice sizes of 1/50, 1/70, 1/90, 1/110, and 1/130, as shown in

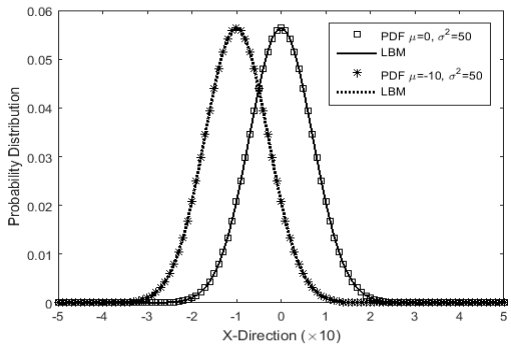

Fig. 3. Probability distribution function at different initial concentrations.

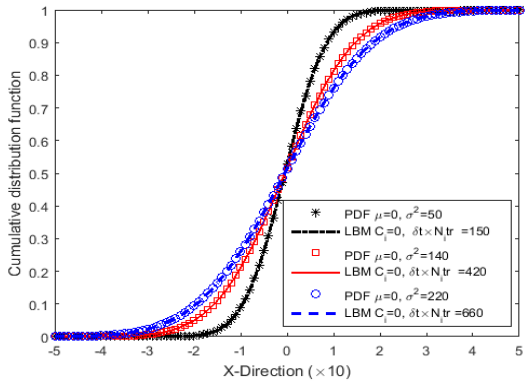

(a)

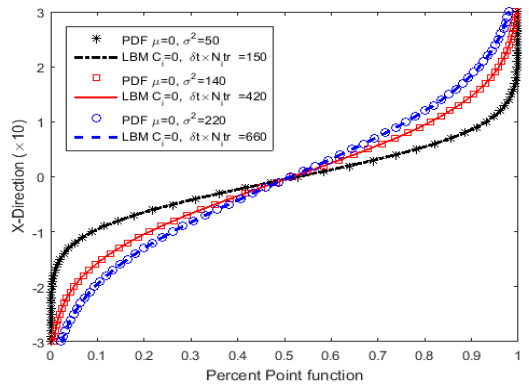

(b)

Fig. 4. The cumulative distribution function (a) and the percent point function (b) at different variance.

Table 1. Fig. 5 and the table show that the CIP-LBM scheme for the CDE is second-order accurate in space, and smaller error is obtained with smaller lattice size. Also, the relative errors of the smaller lattice nodes increase faster in time, while there is no ostensible growth for smaller lattice size.

Table 1. Relative errors of the scalar variable ϕ with different lattice size

δ_x	Err_{lb}
7.70×10^{-3}	1.56×10^{-4}
9.10×10^{-3}	1.35×10^{-3}
1.11×10^{-2}	8.68×10^{-3}
1.43×10^{-2}	4.21×10^{-3}
2.00×10^{-2}	1.64×10^{-2}

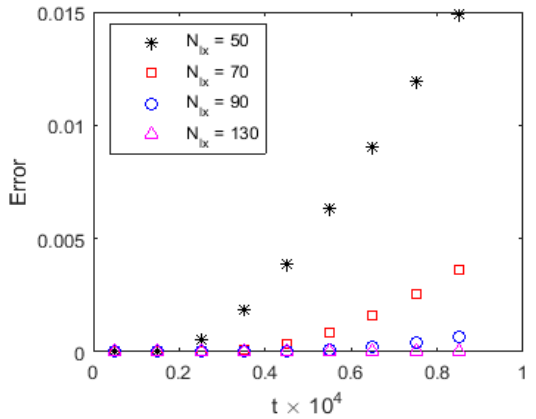

Fig. 5. Relative errors of ϕ at different times

3.2 Bounded and unbounded plane sheet

In this example, we first consider one-dimensional diffusion in a finite domain of length L and in which all the diffusing substance is initially concentrated in a plane. In a bounded domain, the curve reflected at $x = L/2$ is reflected again at $x = 0$. The initial condition is that there is no flow of diffusing substance through the surface, which can be defined as:

$$\frac{\partial \phi}{\partial x} = 0, \quad x = \frac{L}{2} \quad at\ t = 0 \tag{24}$$

$$\phi = \phi_0\,, \quad h - x \le x \le h + x \quad at\ t = 0 \tag{25}$$

The analytical solution of the infinite domain in diffusion can be obtained by applying the Laplace transform method:

$$\phi = \phi_i + \frac{1}{2}\phi_0 \sum_{-\infty}^{+\infty} \left\{ \begin{array}{l} \mathrm{erf}\left[\dfrac{h + nL - x}{2(Dt)^{-1/2}}\right] \\ +\mathrm{erf}\left[\dfrac{h - nL + x}{2(Dt)^{-1/2}}\right] \end{array} \right\} \tag{26}$$

where ϕ_i is the uniform initial concentration, and the infinite sum of the error function represents a superposition of the original diffusion process at the boundaries.

The D1Q3 scheme of LBM was applied in simulations. The simulations were paused after reaching a chosen time, and the LBM parameters are $\tau_\phi = 1$, $\phi_i = 0$, and $\phi_0 = 1$. A lattice size of 1/100 was fine enough to obtain accurate results. The numerical and exact solutions of the problem are presented in Fig. 6, which shows that CIP-LBM has good agreement with the analytical results.

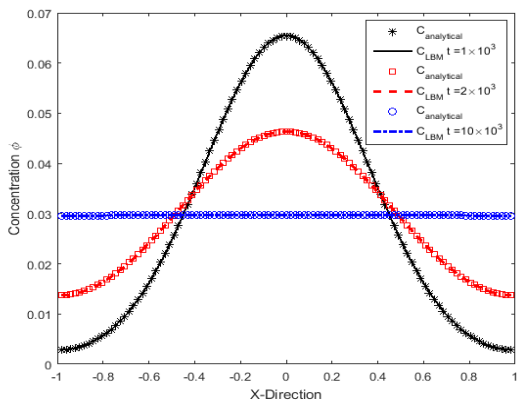

Fig. 6. Concentration distributions for a finite domain.

After validation, we carried out a simulation of the bounded domain in two dimensions using the D2Q5 scheme (a two-dimensional scheme with five velocity vectors). The LBM parameters are $\tau_\phi = 1$, $\phi_i = 0$, and $\phi_0 = 1$. The lattice size was set as 51 × 51, and an interpolated boundary condition was used in the horizontal and vertical boundaries. Fig. 7–10 show images of the process for different times.

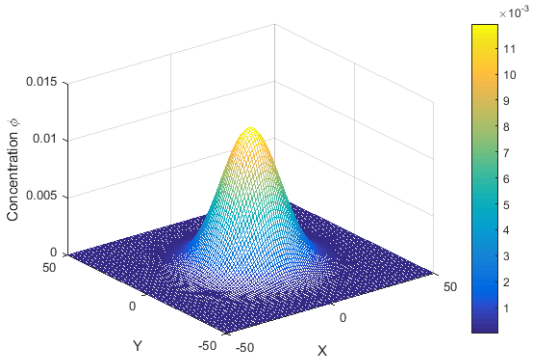

Fig. 7. Concentration distributions for a finite domain, t = 400δt.

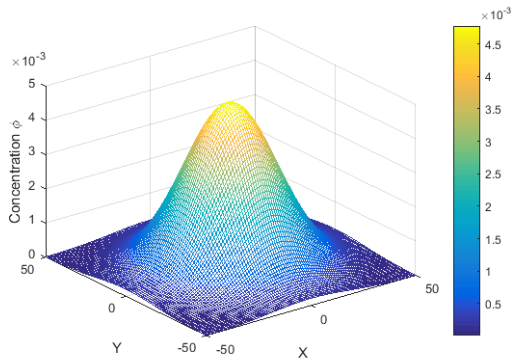

Fig. 8. Concentration distributions for a finite domain, t = 850δt.

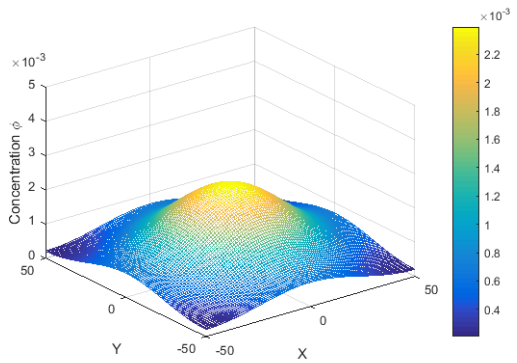

Fig. 9. Concentration distributions for a finite domain, t = 2000δt.

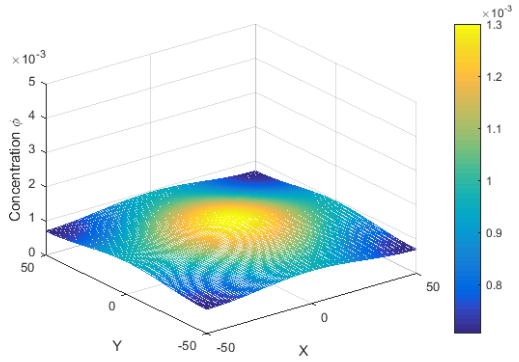

Fig. 10. Concentration distributions for a finite domain, t = 4000δt.

3.3 Poiseuille flow

Poiseuille flow is the last problem tested to demonstrate the capability of the present model for solute transport. In this simulation, the flow rate is given by a pressure drop or an external force with constant density and acceleration in the x direction, along which gravity acceleration acts. The bottom and top walls are fixed, and developed flow passes through the channel from the left and goes out from the right boundary condition. The maximum velocity is u_0 can occur in the center of the inlet boundary, while the velocity in the y direction is zero. Also, a constant concentration boundary condition is used for the top ($\phi_l = 1$) and bottom ($\phi_0 = 0$) walls. In LBM, the bounce back boundary condition is used for the top and bottom walls, and a periodic boundary condition is applied for the left and right walls. The analytical solution of the Poiseuille flow is[4]:

$$u = \frac{g_x H y}{2\nu}\left(1 - \frac{y}{H}\right) \quad where\ g_x \neq 0$$
$$\phi = \phi_0 + (\phi_1 - \phi_0)\frac{y}{H} \tag{28}$$

where H is the height of the channel, and ϕ_0 and ϕ_l are the constant values of the scalar variable of concentration on the top and bottom walls. The

Peclet and Reynolds numbers are:

$$e = \frac{HU_{max}}{\nu}, \quad Pe = \frac{HU_{max}}{D} \tag{29}$$

where the maximum velocity that occurs in the center of the channel (H/2) in steady conditions is given by:

$$U_{max} = \frac{g_x H^2}{8\nu} \tag{30}$$

We applied the D2Q9 scheme to perform several simulations at different Reynolds and Peclet numbers. Fig. 11(a) and 11(b) show that the numerical results are in excellent agreement with the analytical solution. For quantitative study on the deviation between the proposed method and the analytical solution, statistical analysis related to the relative error was preformed, and the results are presented in Fig. 12(a) and 12(b). It is clear from these Figures that the accuracy of the simulation is higher for smaller lattice size and small Peclet number, and the numerical results of concentration perfectly match the exact solution.

4. Conclusions

We have proposed the CIP-LBM method for solving the CDE. We carried out different simulations of one-dimensional problems such as bounded domain and modeling the probability distribution function by using the LBM. The LBM has high capability to solve this type of problem because only the bounce back boundary condition is suitable for a diffusion process if no flux boundary is required. This advantage of using LBM is significant for diffusion simulation, especially in porous media, because applying specific solute boundary conditions is not required at solid-fluid interfaces, and using a bounce back

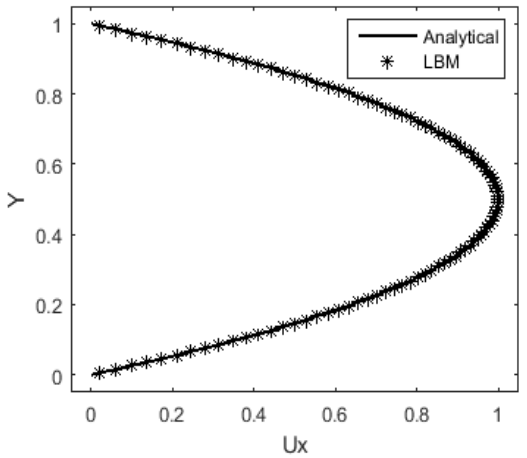

(a)

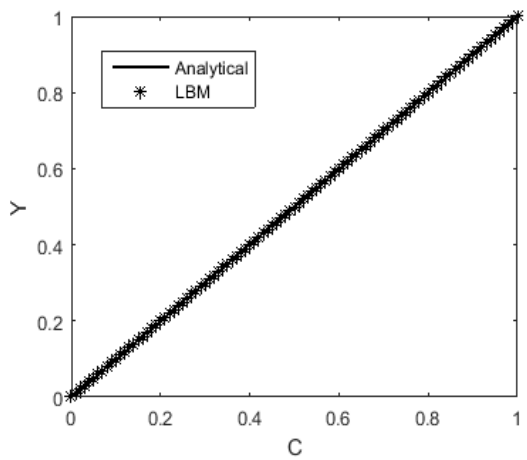

(b)

Fig. 11. (a) Velocity profile for gravity-driven flow, Re = 10 and Pe =1. (b) Distributions of concentration along the y direction

boundary condition is very simple.

A two-dimensional diffusion problem in the Poiseuille flow was also performed and compared with the corresponding analytical solutions. The relative errors of the concentration variable ϕ decreased with the increase of lattice size, but they have an opposite trend with increases in Peclet number. The validation exercises demonstrate that the present model has excellent agreement with the analytical solution, and CIP-LBM is expected to solve mass transfer problems with complex geometries.

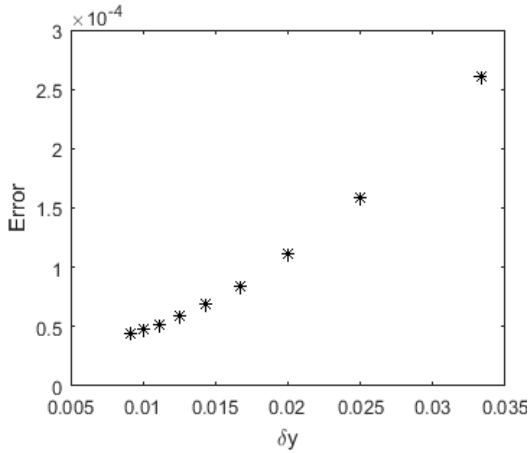

(a)

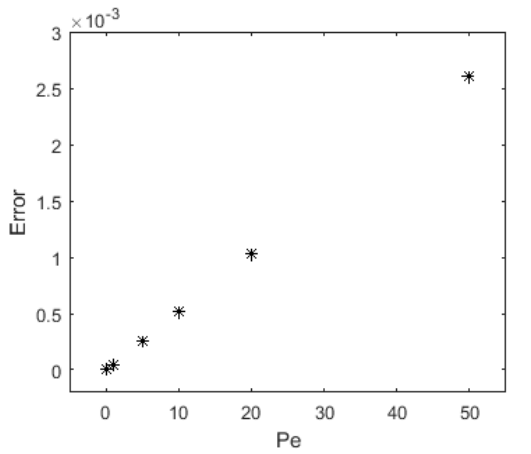

(b)

Fig. 12. (a) Relative error between different lattice size, Re = 10, Pe=1 (b) Relative error between different Peclet number, Re=10

Acknowledgements

This work was supported by the National Research Foundation of Korea (NRF) grant, which is funded by the Korean government (MSIT) (No. 2020R1A5A8018822, No. 2021R1C1C2009287).

REFERENCE

1) Ponce Dawson, S., S. Chen, and G.D. Doolen, Lattice Boltzmann computations for reaction-diffusion equations. The Journal of Chemical Physics, 1993. 98(2): p. 1514-1523.
2) Sukop, M.C. and D.T. Thorne, Lattice Boltzmann Modeling: An Introduction for Geoscientists and Engineers. 2010: Springer Publishing Company, Incorporated. 172.
3) Benzi, R., S. Succi, and M. Vergassola, The lattice Boltzmann equation: theory and applications. Physics Reports, 1992. 222(3): p. 145-197.
4) Chai, Z. and T.S. Zhao, Lattice Boltzmann model for the convection-diffusion equation. Physical Review E, 2013. 87(6): p. 063309.
5) van der Sman, R.G.M. and M.H. Ernst, Convection-Diffusion Lattice Boltzmann Scheme for Irregular Lattices. Journal of Computational Physics, 2000. 160(2): p. 766-782.
6) Safdari, A. and K.C. Kim, Lattice Boltzmann simulation of the three-dimensional motions of particles with various density ratios in lid-driven cavity flow. Applied Mathematics and Computation, 2015. 265: p. 826-843.
7) Mussa, M.A., et al., Simulation of natural convection heat transfer in an enclosure by the lattice-Boltzmann method. Computers & Fluids, 2011. 44(1): p. 162-168.
8) Ginzburg, I., Equilibrium-type and link-type lattice Boltzmann models for generic advection and anisotropic-dispersion equation. Advances in Water Resources, 2005. 28(11): p. 1171-1195.
9) Shan, X., Simulation of Rayleigh-Benard convection using a lattice Boltzmann method. Physical Review E, 1997. 55(3): p. 2780-2788.
10) McNamara, G. and B. Alder, Analysis of the lattice Boltzmann treatment of hydrodynamics. Physica A: Statistical Mechanics and its Applications, 1993. 194(1–4): p. 218-228.
11) Zhaoli Guo, T.S. Zhao, Lattice Boltzmann simulation of natural convection with temperature-dependent viscosity in a porous cavity. Progress in Computational Fluid Dynamics, An International Journal, 2005. 5(1/2): p. 110-117.

12) Zhou, J.G., A lattice Boltzmann method for solute transport. International Journal for Numerical Methods in Fluids, 2009. 61(8): p. 848-863.
13) Safdari, A. and K.C. Kim, Lattice Boltzmann simulation of solid particles behavior in a three-dimensional lid-driven cavity flow. Computers & Mathematics with Applications, 2014. 68(5): p. 606-621.
14) Deng, B., B.-C. Shi, and G.-C. Wang, A New Lattice Bhatnagar–Gross–Krook Model for the Convection–Diffusion Equation with a Source Term. Chinese Physics Letters, 2005. 22(2): p. 267.
15) Takewaki, H., A. Nishiguchi, and T. Yabe, Cubic interpolated pseudo-particle method (CIP) for solving hyperbolic-type equations. Journal of Computational Physics, 1985. 61(2): p. 261-268.
16) Gomberg, J., et al., Time-dependent earthquake probabilities. Journal of Geophysical Research: Solid Earth, 2005. 110(B5): p. n/a-n/a.
17) Ring, A., et al., Sensitivity of Empirical Metrics of Rate of Absorption in Bioequivalence Studies. Pharmaceutical Research, 2000. 17(5): p. 583-588.
18) Ren, X., D. Yan, and C. Wang, Air-conditioning usage conditional probability model for residential buildings. Building and Environment, 2014. 81: p. 172-182.